All-Optical Reshaping Based on a Passive Saturable Absorber Microcavity Device for Future 160-Gb/s Applications

Julien Fatome, Stphane Pitois, Aladji Kamagaté, Guy Millot, David Massoubre, Jean-Louis Oudar

All-optical reshaping based on a passive saturable absorber microcavity device for future 160-Gbit/s applications

J. Fatome, S. Pitois, A. Kamagate and G. Millot

Laboratoire de Physique de l'Université de Bourgogne - LPUB - CNRS UMR5027
9 av. Alain Savary, 21078 Dijon, France

D. Massoubre and J. L. Oudar

Laboratory for Photonic and Nanostructures - LPN - CNRS UPR20
Route de Nozay, 91460 Marcoussis, France

(May 03, 2006)

Abstract

A vertical-access passive all-optical switching gate has been used to regenerate the zero levels of a "…01010101…" 160-Gbit/s bit pattern at 1561 nm. Autocorrelation function measurements show that an extinction up to 11.7 dB of the "ghost-pulses" can be achieved.

Keywords: Optical 2R regeneration, Optical communication, Fabry-Perot microcavity, Switching gate, Saturable absorber, Ultrashort pulses, Nonlinear Optics, Autocorrelation.

I. INTRODUCTION

In the next-generation of transmission systems and in particular in future upgrading of the already installed fiber-optic networks to higher time-division-multiplexed (TDM) bit rates, picosecond and even subpicosecond pulses will be transmitted through optical fibers [1-2]. Consequently, impairments due to nonlinear, dispersion or polarization mode dispersion effects will be dramatically increased, severely limiting the propagation distance. Thus, in order to develop such future networks, and in a present context of bit-cost reduction, there is a growing demand for low-cost ultra high-speed all-optical regenerators capable to combat cumulative transmission impairments such as the generation of "ghost-pulses" in the "0" bit slots due to the combined effects of both dispersion and nonlinearities [3]. Some preliminary experiments of signal reshaping at 160 Gbit/s have already been successfully done in back-to-back configurations by means of Nonlinear Optical Loop Mirrors (NOLM) [4] and Saturable Optical Amplifiers (SOA) [5]. But it is well known that NOLMs generally suffer from a complex experimental setup, require very strong input energies and are strongly dependent on signal polarisation and fiber parameters; while SOAs are active components and based on a wavelength conversion process. On the other hand, the Saturable Absorber (SA) device is totally passive, polarisation independent, easy to use, its relaxation time can be adjusted to less than 1 ps [6] and one may reshape several wavelengths on the same chip [7], making it more suitable for low cost reshaping. Moreover, benefits of quantum well microcavity SA have already been demonstrated through 10-Gbit/s and 40-Gbit/s long haul transmission recirculating loop experiments [7, 8] and also by improving the extinction ratio of a 160-GHz pulse source using a 1-ps relaxation time component [9]. In this letter, the regenerative capabilities of such a saturable absorber-based microcavity device are investigated for the first time to our knowledge for future 160-Gbit/s applications. In this aim, a degraded "…01010101…" 160-Gbit/s bit pattern combined with autocorrelation function measurements have been used to characterize the regenerative properties of our saturable absorber component.

II. DESIGN AND FABRICATION OF THE DEVICE

The structure reported in this paper and its principle of operation are similar to the ones reported elsewhere [7-11]. It consists of an active layer (7 InGaAs/InP quantum wells)

comprised inside an asymmetric Fabry-Perot micro-cavity and suitably located at the antinodes of the intracavity intensity. After MOVPE growth, the structure underwent 12°MeV Ni^{6+} ion irradiation with a dose of $1x10^{12}$ cm^{-2}. Such energetic ions create clusters of defects along the ion path through the active layer. These defects act as carrier recombination centers, which shorten the carrier lifetime down to a few picoseconds [6]. Pump and probe measurement at 1555 nm showed a response time of 1 ps and already published results on the experimental reshaping of a 160-GHz pulse train have demonstrated that the response time of this SA device is fully compatible with 160-Gbit/s applications [9]. The back mirror was made by the deposition of a thin silver (Ag) layer, then a top-down mounting was made by soldering this Ag film on a silicon wafer by means of an In-Au metallic bonding to improve the heat dissipation. A finely controlled chemical etching of the top InP phase layers permitted the resonance matching with the quantum well excitonic absorption wavelength. The microcavity resonance has a typical –3 dB bandwidth of 50 nm centered at 1.55 µm. Finally a two period dielectric layer (2x SiO_2/TiO_2 : $\lambda/4$ / $\lambda/4$) was deposited as front mirror of the cavity. The cavity was designed to have a reflectivity close to zero at low intensity (impedance matching).

III. EXPERIMENTAL RESULTS AND DISCUSSION

The experimental setup is shown in Fig. 1. A high quality 80-GHz 2.4-ps transform-limited pulse train was first generated at 1561 nm by using the multiple four wave mixing technique in a 1420-m long Teraligth fiber [12]. Then, a 50:50 coupler combined with a 6.25 ps delay line was used to generate through multiplexing in the time domain, the following simplified bit pattern "…01010101…" at 160-Gbit/s. A variable attenuator (Att) has also been inserted into the delay line in order to adjust the energy of the ghost-pulses injected into the "0" bit slots. The resulting poor quality 160-Gbit/s pulse train was then amplified by means of an Erbium doped fiber amplifier (EDFA) and focused on the microcavity saturable absorber (SA) device thanks to a fiber-pigtailed high aperture lens producing a focus spot of 5 µm diameter at $1/e^2$ of the maximum intensity (the insertion losses of the regenerative module were evaluated to 10 dB). Finally, the signal at the SA input and the corresponding regenerated pulse train at the SA output were recorded by means of a second-harmonic background-free autocorrelator. Figure 2a represents in a logarithm scale the output autocorrelation traces of the bit pattern as a function of the input average power focused on

the device. The Curve (1) in dashed line corresponds to the initial "…01010101…" 160-Gbit/s bit pattern recorded at the output of the delay line. After reflection on the SA device, we can clearly observe a large improvement of the signal quality as the input average power increases. This improvement is characterized by a strong reduction of the energy contained in the "0" bit slots with nearly an extinction of these ghost-pulses for an average power close to 80 mW (curve 4). Figure 2b illustrates the evolution with respect to the SA input average power of both the intensity extinction ratio (IER) improvement (circles) and the relative amount of energy, E_r (stars), contained in the ghost-pulses; and defined as the ratio between the energy contained in the "0" slots and the total energy. IER and E_r are given here by:

$$IER=-10\ log\left(\frac{R_{out}}{R_{in}}\right), \tag{1}$$

$$\text{with } R=\frac{E_0}{E_1}, \tag{2}$$

where E_0 and E_1 are the energy contained in the ghost-pulses and in the "1" slots respectively,

and

$$E_r=\frac{E_0}{E_0+E_1}, \tag{3}$$

with E_0+E_1 the total energy.

We can see on Fig. 2b that the optimum SA input average power for which the highest pulse quality improvement is observed, was measured to be 80 mW (19 dBm). With this experimental configuration, the IER enhancement is maximal and equal to 11.7 dB, leading to a drop of the relative amount of energy contained in the "0" slots from E_r = 10.5 % to only E_r = 0.8 %. Note that when the power is increased above 80 mW the IER enhancement decreases significantly, owing to a thermal shift of the spectral resonance with increasing average power [11]. A second series of experiments was carried out to test the regenerative efficiency of our SA device as a function of the ghost-pulse input energy. Figures 3a and 3b represent the input (circles) and output (solid line) autocorrelation functions of the 160-Gbit/s sequence for an initial ratio of energy injected into the "0" slots of E_r = 3.7 % (Fig. 3a) and E_r = 19.6 % (Fig. 3b). After reshaping in the SA device at the optimum input average power, no dramatic change was noticed on the bits "1", except a small temporal compression from 2.46 ps to 2.30 ps. Note that Frequency Resolved Optical Gating (FROG) characterizations made on a 1.3-ps 160-GHz pulse train [9] have shown that a slight asymmetry could also be introduced

by our component on the pulse intensity profile because of a pulse width comparable to the response time of our component. This phenomenon is hidden because of the symmetric feature of the autocorrelation function but should be negligible here because of a pulse width (2.4 ps) more than twice larger than the response time (1 ps). On the other hand, we can clearly observe a strong reduction of the ghost-pulses contained in the "0" bit slots which relative amount of energy decreased to E_r = 0.5 % in Fig. 3a and to E_r = 3.4 % in Fig. 3b, confirming the saturable regenerative action of our component. Figure 4a sums up all the "0" bit reshaping measurements. In this figure, we plot the nonlinear response of our SA device, i.e. the output ratio of energy E_r contained in the ghost-pulses as a function of the input ratio. As expected, our SA device is characterized by a nonlinear response with a large discrimination of low powers which is essential for any all-optical regeneration processing. These results complete our previous work in the sense that the SA device is now proved to be able to reshape not only consecutive "1s" cadenced at 160 GHz [9] but also a sequence made of a "0" level followed or preceded by a "1", and separated by 6.25 ps. This is a strong indication that our SA component is compatible with future 160-Gbit/s regeneration applications. Finally, in order to complete the characterization of our SA device, we measured its sensitivity to possible patterning effects caused by transient thermal phenomena by recording the spectral resonance shift as a function of the 160-Gbit/s pattern length for a fixed input average power. For these measurements, we used an acousto-optic switch at the input of the SA device in order to adjust the sequence length and its duty-cycle. Figure 4b represents the experimental results obtained for a pattern length ranging from 100 ns to 10 ms and for an adjusted duty-cycle of 4 ensuring a constant average power at the device input. We can see that after a rough increase of the resonance shift, the spectral resonance stabilizes around 1561 nm from a pattern length of 100 µs, indicating that the characteristic time of thermal effects can be estimated to be 6 orders of magnitude larger than the bit slot duration (~10 µs compared to 6.25 ps). Consequently, assuming that the rising and decreasing times of thermal effects are equal, in the case of a pseudo-random bit sequence, the rapid changes of pattern even with long series of "1" or "0" will do not significantly shift the resonance wavelength of our component and thus, will not affect its regeneration efficiencies.

IV. CONCLUSION

In this paper, we have investigated the regeneration capabilities of a passive and all-optical saturable absorber-based switching gate for future 160-Gbit/s reshaping applications. A "…01010101…" 160-Gbit/s pattern was generated by multiple four wave mixing and time multiplexing at 1561 nm and used as degraded signal for the regenerative characterizations. Autocorrelation function measurements show that a reduction up to 11.7 dB of the energy contained in the ghost-pulses can be achieved for an input average power of 80 mW (19 dBm). Moreover, we have shown that the thermal effects are sufficiently slow compared to the bit slot duration and consequently that any patterning effects should not affect its regeneration capabilities. These results have to be confirmed by a pseudo-random bit sequence 160-Gbit/s experiment but they already indicate that this device is a promising candidate for future low-cost all-optical 2R-regeneration at 160-Gbit/s.

References

[1] H.G. Weber, S. Ferber, M. Kroh, C. Schmidt-Langhorst, R. Ludwig, V. Marembert, C. Boerner, F. Futami, S. Watanabe and C. Schubert, **"**Single channel 1.28 Tbit/s and 2.56 Tbit/s DQPSK transmission", Elecron. Lett., 42, pp. 178-179, 2006.

[2] A. H. Gnauck, G. Raybon, P. G. Bernasconi, J. Leuthold, C. R. Doerr and L. W. Stulz, "1-Tb/s (6 x 170.6 Gb/s) Transmission Over 2000-km NZDF Using OTDM and RZ-DPSK Format", Photon. Technol. Lett., 15, pp. 1618-1620, 2003.

[3] R.-J. Essiambre, B. Mikkelsen and G. Raybon, "Intra-channel cross-phase modulation and four-wave mixing in high-speed TDM systems", Electron. Lett., 35, pp. 1576-1578, 1999.

[4] A. Bogoni, P. Ghelfi, M. Scaffardi and L. Poti, "All-Optical Regeneration and Demultiplexing for 160-Gb/s Transmission Systems using NOLM-Based Three-Stage Scheme", IEEE J. Select. Topics Quant. Electron., 10, pp 192-195, 2004.

[5] J. Leuthold, L. Möller, J. Jaques, S. Cabot, L. Zhang, P. Bernasconi, M. Cappuzzo, L. Gomez, E. askowski, E. Chen, A. Wong-Foy and A. Griffin "160 Gbit/s SOA all-optical wavelength converter and assessment of its regenerative properties", Electron. Lett., 40, pp. 554-555, 2004.

[6] L. Joulaud, J. Mangeney, G. Patriarche, J.-M. Lourtioz, and P. Crozat, "Thermal stability of ion-irradiated InGaAs with (sub-) picosecond carrier lifetime", Appl. Phys. Lett., 82, pp. 856-858, 2003.

[7] D. Rouvillain, F. Seguineau, L. Pierre, P. Brindel, H. Choumane, G. Aubin, J.-L. Oudar, and O. Leclerc, "Optical 2R regenerator based on passive saturable absorber at 40 Gbit/s for WDM long haul transmissions", Electron. Lett., 38, pp. 1113-1114, 2002.

[8] M. Gay, L. Bramerie, D. Massoubre, A. O'Hare, A. Shen, J.L. Oudar and J.C. Simon, "Cascadability Assessment of a 2R Regenerator Based on Saturable Absorber and Semiconductor Optical Amplifier in a Path Switchable Recirculating Loop", Photon. Techno. Lett., 18, pp 1273-1275, 2006.

[9] D. Massoubre, J.-L. Oudar, J. Fatome, S. Pitois, G. Millot, J. Decobert and J. Landreau, "All-optical extinction ratio enhancement of a 160 GHz pulse train using a saturable absorber vertical microcavity", Opt. Lett., 31, pp. 537-539, 2006.

[10] D. Massoubre, J.-L. Oudar, J. Dion, J.-C. Harmand, A. Shen, J. Landreau and J. Decobert, "Scaling of the saturation energy in microcavity saturable absorber devices", Appl. Phys. Lett., 88, 153513, 2006.

[11] D. Massoubre, J.-L. Oudar, A. O'Hare, M. Gay, L. Bramerie, J.-C. Simon, A. Shen, and J. Decobert, "Analysis of Thermal Limitations in High-Speed Microcavity Saturable Absorber All-Optical Switching Gates", J. Lightw. Technol., vol. 24, no. 9, pp 3400-3408, 2006.
[12] J. Fatome, S. Pitois and G. Millot, "20-GHz to 1-THz repetition rate pulse sources based on multiple four wave mixing in optical fibers", IEEE J. Quant. Electron., 42, pp. 1038-1046, 2006.

Figure Captions

Fig. 1: Experimental setup. Att: variable optical attenuator, $\Delta\tau$: delay line, EDFA: Erbium doped fiber amplifier, SA: saturable absorber.

Fig. 2: (a) Autocorrelation functions of the 160-Gbit/s pattern as a function of the SA input average power. (1) SA input reference, (2) 60 mW (17.8 dBm), (3) 70 mW (18.5 dBm), (4) 80 mW (19 dBm) **(b)** Intensity extinction ratio (ER) improvement (circles) and ratio of energy E_r contained in the ghost-pulses at the SA output (stars) as a function of the input average power.

Fig. 3: Autocorrelation functions of the 160-Gbit/s sequence at the input (circles) and output (solid lines) of the SA device. **(a)** In: E_r=3.7 %, out: E_r=0.5 % and **(b)** In: E_r=19.6 %, out: E_r=3.4 %, respectively.

Fig. 4: (a) Nonlinear response of our SA device: ratio of energy E_r contained in the ghost-pulses at the output of the SA device as a function of the input ratio **(b)** Resonance wavelength as a function of the sequence length.

J. Fatome et al. Figure 1

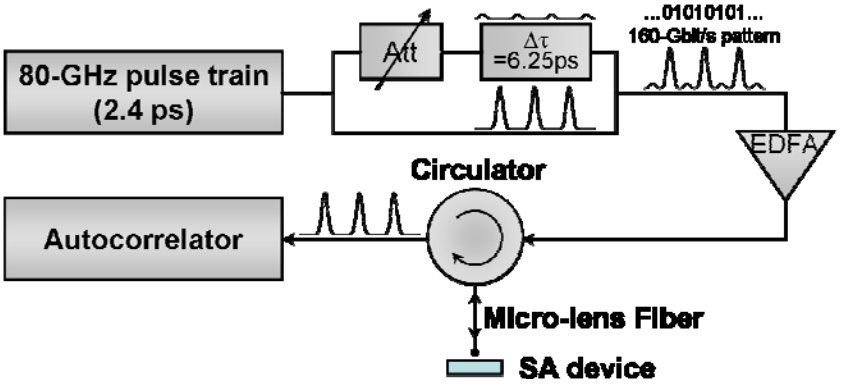

Fig. 1: *Experimental setup. Att: variable optical attenuator, Δτ: delay line, EDFA: Erbium doped fiber amplifier, SA: saturable absorber.*

J. Fatome et al. Figure 2

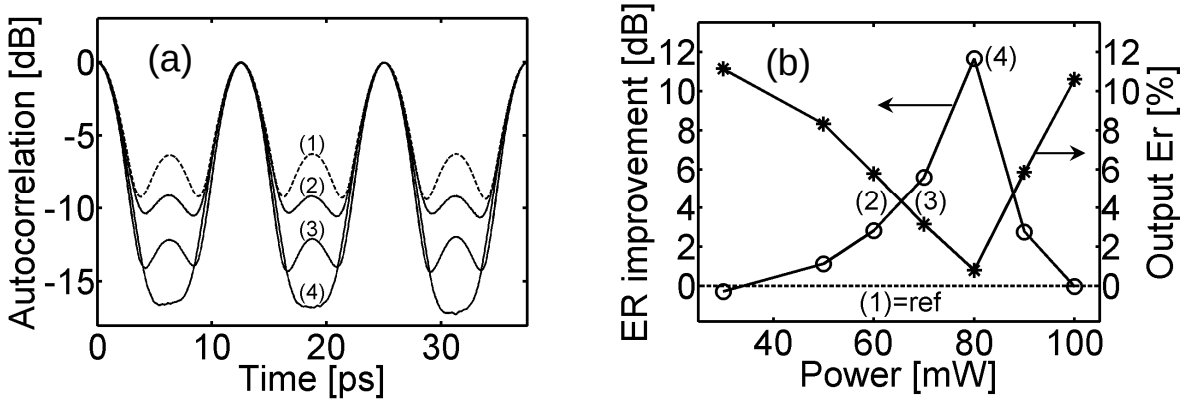

Fig. 2: (a) *Autocorrelation functions of the 160-Gbit/s pattern as a function of the SA input average power. (1) SA input reference, (2) 60 mW (17.8 dBm), (3) 70 mW (18.5 dBm), (4) 80 mW (19 dBm)* ***(b)*** *Intensity extinction ratio (ER) improvement (circles) and ratio of energy E_r contained in the ghost-pulses at the SA output (stars) as a function of the input average power.*

J. Fatome et al. Figure 3

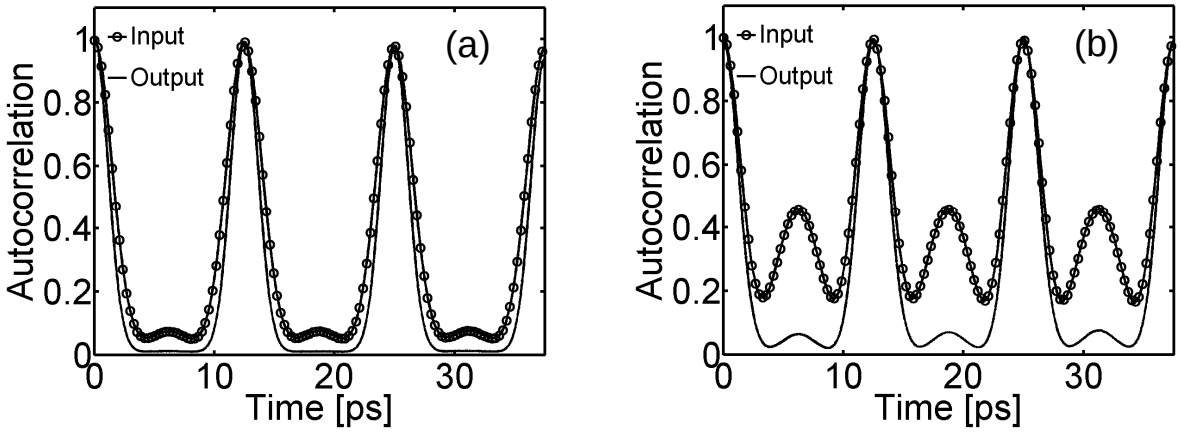

Fig. 3: *Autocorrelation functions of the 160-Gbit/s sequence at the input (circles) and output (solid lines) of the SA device.* ***(a)*** *In: E_r=3.7 %, out: E_r=0.5 % and* ***(b)*** *In: E_r=19.6 %, out: E_r=3.4 %, respectively.*

J. Fatome et al. Figure 4

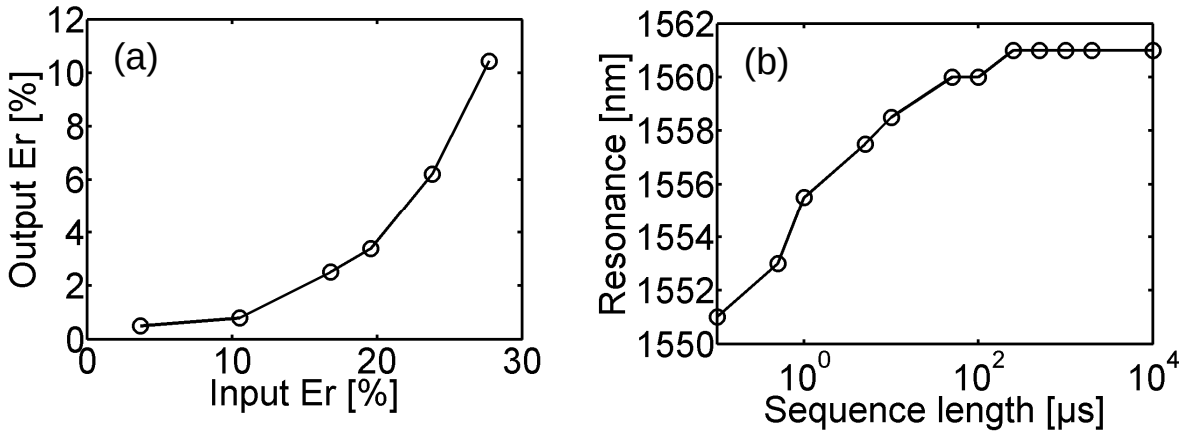

Fig. 4: (a) *Nonlinear response of our SA device: ratio of energy E_r contained in the ghost-pulses at the output of the SA device as a function of the input ratio* ***(b)*** *Resonance wavelength as a function of the sequence length.*